

## Simulating Surface Energy Fluxes and Radiometric Surface Temperatures for Two Arid Vegetation Communities Using the SHAW Model

G. N. FLERCHINGER

*Northwest Watershed Research Center, USDA Agricultural Research Service, Boise, Idaho*

W. P. KUSTAS

*Hydrology Lab, USDA Agricultural Research Service, Beltsville, Maryland*

M. A. WELTZ

*Southwest Watershed Research Center, USDA Agricultural Research Service, Tucson, Arizona*

(Manuscript received 4 March 1997, in final form 8 August 1997)

### ABSTRACT

While land-atmosphere transfer models have been pursued for over 30 years, Soil-Vegetation-Atmosphere-Transfer (SVAT) models are gaining attention only recently as the need to better represent the interaction between the soil and atmosphere in atmospheric circulation models becomes more apparent. The Simultaneous Heat and Water (SHAW) model, a detailed physical process model, simulates the effects of a multispecies plant canopy on heat and water transfer at the soil-atmosphere interface. The model was used in this study to simulate the surface energy balance and surface temperature of two vegetation communities using data collected during the Monsoon '90 multidisciplinary field experiment. The two vegetation communities included a sparse, relatively homogeneous, grass-dominated community and a shrub-dominated site with large bare interspace areas between shrubs. The model mimicked the diurnal variation in the surface energy balance at both sites, while canopy leaf temperatures were simulated somewhat better at the relatively homogeneous grass-dominated site. The variation in surface fluxes accounted for by the model (i.e., model efficiency) ranged from 59% for latent heat flux at the shrub-dominated site to 98% for net radiation at both sites. Model efficiency for predicting latent heat flux at the grass-dominated site was 65%. Canopy leaf temperatures for the shrub-dominated site were consistently overpredicted by 1.8°C compared to measured values. Simulated soil surface temperatures at both sites had a model efficiency of 94% and a mean bias error of less than 0.9°C. The ability of the model to simulate canopy and soil surface temperatures gives it the potential to be verified and periodically updated using remotely sensed radiometric surface temperature and soil moisture when extrapolating model-derived fluxes to other areas. A methodology is proposed whereby model predictions can be used with a combination of remotely sensed radiometric surface temperature and surface soil moisture to estimate soil water content within the rooting depth.

### 1. Introduction

Researchers have struggled with describing heat and mass transfer between the atmosphere and vegetated surfaces for 30 years (Waggoner and Reifsnyder 1968). However, transport of mass and energy between the land and atmosphere is an increasing area of interest as the need to better represent surface-atmosphere interactions in climate and atmospheric circulation models becomes apparent. As a result, surface energy balance models, known as Soil-Vegetation-Atmosphere-Transfer (SVAT) models, have been attracting attention as a tool to gain a better under-

standing of this interaction (Henderson-Sellers et al. 1995). Simplified approaches to simulate energy and mass transfer from vegetated surfaces have represented the canopy and underlying substrate as a single source. This approach was shown to be inadequate for areas with sparse vegetation (Blyth and Harding 1995), and many two-source models have been developed (van Bavel et al. 1984; Dickinson et al. 1986; Lascano et al. 1987; Horton 1989; Luo et al. 1992; Massman 1992; Nichols 1992; Huntingford et al. 1995; Inclan and Forkel 1995; Mihailović and Ruml 1996). In general, the two-source SVAT models typically represent the canopy as a single layer and the underlying substrate as a second source, giving much attention to radiation dissipation within the canopy and bulk aerodynamic transfer.

With the expanding availability of remotely sensed data, SVAT models are being developed to use remotely sensed surface soil moisture or radiometric surface temperature

*Corresponding author address:* G. N. Flerchinger, USDA Agricultural Research Service, Northwest Watershed Research Center, 800 Park Boulevard, Suite 105, Boise, Idaho 83712.  
E-mail: gflerchi@nwrc.ars.pn.usbr.gov

as either input or as a validation of the model (Kustas and Norman 1996; Burke et al. 1997). However, the radiometric temperature of a vegetated surface depends on the temperature profile within the canopy and the surface temperature of the substrate (Lagouarde et al. 1995; Norman et al. 1995). To simulate vertical temperature distribution within the canopy and substrate, it becomes necessary to simulate the movement of energy and mass within a canopy (Norman et al. 1995). Waggoner and Reifsnnyder (1968) developed a multilayer canopy approach to simulate temperature and humidity profiles within a plant canopy, but this model required measured net radiation for each canopy layer. As a result, models using a multilayer canopy representation of heat, mass, and radiative transfer have been developed (Sellars et al. 1986; van Griend and van Boxel 1989; Flerchinger and Pierson 1991).

Flerchinger and Pierson (1991) and Flerchinger et al. (1996b) presented additions made to the Simultaneous Heat and Water (SHAW) model to simulate heat and water movement through a multispecies plant canopy using a multilayer representation within the canopy. The SHAW model is a detailed process model that simulates heat and water movement through a plant-snow-residue-soil system and was originally developed by Flerchinger and Saxton (1989) to simulate coupled heat and water movement related to soil freezing and thawing. Flerchinger et al. (1996b) applied the model to simulate surface energy fluxes across a watershed. The purpose of this paper is to further test the ability of the model to simulate the temporal surface energy balance and surface temperatures of different vegetation communities within a semiarid watershed and to explore avenues whereby the model can be used in combination with remotely sensed data. The ability of the model to simulate surface temperature gives it the potential for being periodically updated using satellite observations of radiometric surface temperature, such as that available from NOAA AVHRR (National Oceanic and Atmospheric Administration Advanced Very High Resolution Radiometer) and GOES (Geostationary Operational Environmental Satellite), and to extrapolate model-derived fluxes to basin and regional scales. Because radiometric surface temperature of sparse vegetation is strongly controlled by surface soil moisture, it may be necessary to couple these with remotely sensed surface soil moisture that may be available from microwave radiometers (Schmugge et al. 1994). The model was applied to data collected as part of the Monsoon '90 multidisciplinary field campaign described by Kustas and Goodrich (1994).

## 2. The SHAW model

The physical system described by the SHAW model consists of a vertical, one-dimensional profile extending from the vegetation canopy, snow, residue, or soil surface to a specified depth within the soil (Fig. 1). The system is represented by integrating detailed physics of a plant canopy, snow, residue, and soil into one simultaneous solution, including detailed provisions for soil freezing and

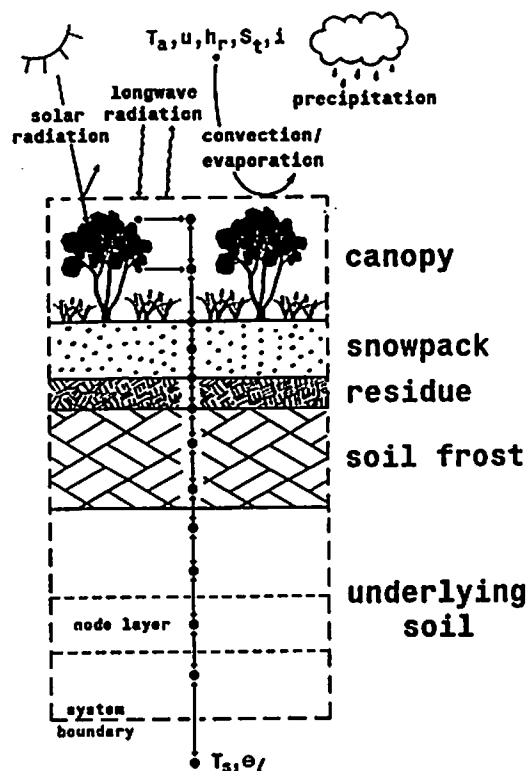


FIG. 1. Physical system described by the SHAW model. ( $T_a$  is temperature,  $u$  is wind speed,  $h$  is relative humidity,  $S_t$  is solar radiation,  $i$  is precipitation,  $T_s$  is soil temperature, and  $\theta$  is water content.)

thawing. Daily or hourly weather conditions above the upper boundary and soil conditions at the lower boundary are used to define heat and water fluxes into the system. A layered system is established through the vegetation canopy, snow, residue, and soil, with each layer represented by a node in a finite-difference representation by which the interrelated heat, liquid water, and vapor fluxes between layers are determined. The model is capable of simulating several different intermixed plant species simultaneously, including standing dead plant material.

### a. Simulation of the surface energy balance

The interrelated energy and water fluxes at the surface boundary are computed from weather observations of air temperature, wind speed, relative humidity, and solar radiation. The surface energy balance may be written as

$$R_n + H + L_v E + G = 0, \quad (1)$$

where  $R_n$  is net all-wave radiation ( $\text{W m}^{-2}$ ),  $H$  is sensible heat flux ( $\text{W m}^{-2}$ ),  $L_v E$  is latent heat flux ( $\text{W m}^{-2}$ ),  $G$  is soil or ground heat flux ( $\text{W m}^{-2}$ ),  $L_v$  is latent heat of evaporation ( $\text{J kg}^{-1}$ ), and  $E$  is total evapotranspiration from the soil surface and plant canopy ( $\text{kg m}^{-2} \text{s}^{-1}$ ), where all fluxes are positive toward the surface.

Net all-wave radiation is determined by computing solar and longwave radiation exchange between canopy layers, residue layers, and the soil surface and consid-

ering direct, and upward and downward diffuse radiation being transmitted, reflected, and absorbed. Transmissivity to radiation for each canopy layer is calculated based on leaf area index and leaf inclination, as described by Flerchinger et al. (1996b). Albedo of the plant leaves are input to the model, and soil surface albedo is related to surface water content. Incoming longwave radiation is computed using input air temperature and an average daily cloud cover estimated from observed solar radiation, as described by Flerchinger et al. (1996a).

Sensible and latent heat flux components of the surface energy balance are computed from temperature and vapor gradients between the canopy-residue-soil surface and the atmosphere. Sensible heat flux is calculated from (Campbell 1977)

$$H = -\rho_a c_a \frac{(T - T_a)}{r_H}, \quad (2)$$

where  $\rho_a$ ,  $c_a$ , and  $T_a$  are the density ( $\text{kg m}^{-3}$ ), specific heat ( $\text{J kg}^{-1} \text{ } ^\circ\text{C}^{-1}$ ), and temperature ( $^\circ\text{C}$ ) of the air at reference height  $z_r$ ;  $T$  is the temperature ( $^\circ\text{C}$ ) of the exchange surface, taken as air temperature within the first canopy layer; and  $r_H$  is the resistance to heat transfer ( $\text{s m}^{-1}$ ) corrected for atmospheric stability. Latent heat flux associated with transfer of water vapor from the exchange surface to the atmosphere is given by

$$L_v E = -L_v \frac{(\rho_v - \rho_{va})}{r_v}, \quad (3)$$

where  $\rho_v$  and  $\rho_{va}$  are vapor density ( $\text{kg m}^{-3}$ ) of the exchange surface and at the reference height, and the resistance value for vapor transfer,  $r_v$ , is taken to be equal to  $r_H$ . Further details of sensible and latent heat transfer are given by Flerchinger et al. (1996b).

Ground heat flux, computed from the residual of the energy balance, must satisfy the solution of the heat flux equations for the entire residue/soil profile, which is solved simultaneously and iteratively with the surface energy balance. Heat and water flux equations for canopy, snow, residue, and soil layers are written in implicit finite difference form and solved using an iterative Newton-Raphson technique. Partial derivatives of the flux equations with respect to the unknown end-of-time-step values are computed from which the Newton-Raphson approximations for the unknown values are computed. Iterations are continued until successive approximations of temperature and water (vapor density within the canopy and residue, and water potential in the soil) are within a prescribed tolerance defined by the user. Details of heat and water flux equations for the residue and soil are given by Flerchinger and Saxton (1989).

#### b. Processes within the canopy

Heat and vapor fluxes within the canopy are determined by computing transfer between layers of the can-

opy and considering the source terms for heat ( $H_{i,i}$ ) and transpiration ( $E_{i,i}$ ) from the canopy leaves for each layer ( $i$ ) within the canopy. Gradient-driven transport, or K theory, is used for transfer within the canopy. Lagrangian approaches for modeling turbulent transport processes within the canopy have been successfully applied by some (e.g., Raupach 1989) as an alternative to K theory since studies indicate that K theory is not applicable in the canopy air space (Denmead and Bradley 1985). However, Lagrangian approaches are not yet ready for general application as further details need to be worked out, for example, limitations in simulating nighttime fluxes. Nevertheless, many have found K theory particularly useful for simulating transport processes within the canopy (van de Griend and van Boxel 1989; Goudriaan 1989; Nichols 1992; Huntingford et al. 1995), while other studies indicate relatively small differences in flux predictions between Lagrangian and K theory (e.g., Dolman and Wallace 1991). Thus, heat flux and temperature within the air space of the canopy is described by

$$\frac{\partial}{\partial z} \left( \rho_a c_a k_r \frac{\partial T}{\partial z} \right) + H_i = \rho_a c_a \frac{\partial T}{\partial t}, \quad (4)$$

where  $z$  is height above the soil surface (m),  $k_r$  is a transfer coefficient within the canopy ( $\text{m}^2 \text{ s}^{-1}$ ), and  $H_i$  is heat transferred from the vegetation elements (leaves) to the air space within the canopy ( $\text{W m}^{-3}$ ). (The above equation does not include the adiabatic lapse rate, which is negligible for the vertical distances considered in the model; additionally, the heat storage term included in the above equation is negligible and not considered in the model.) Vapor flux through the canopy is written similarly to the heat flux equation:

$$\frac{\partial}{\partial z} \left( k_r \frac{\partial \rho_v}{\partial z} \right) + E_i = \frac{\partial \rho_v}{\partial t}, \quad (5)$$

where  $E_i$  is transpiration from the leaves within the canopy ( $\text{kg s}^{-1} \text{ m}^{-3}$ ). Transfer of heat and vapor within the canopy is dependent upon location within the canopy, and several approaches for computing the transfer coefficient  $k_r$  have been developed. Flerchinger and Piereson (1991) used the following expression above the zero plane displacement  $d$ :

$$k_r = k u_* (z - d + z_H) / \phi_h, \quad (6)$$

and for heights less than  $d$ ,

$$k_r = k u_* z_H / \phi_h, \quad (7)$$

where  $k$  is von Kármán's constant,  $u_*$  is the friction velocity ( $\text{m s}^{-1}$ ),  $z$  is height above the residue or soil surface (m),  $d$  is the height of the zero plane displacement (m),  $z_H$  is the thermal surface roughness parameter (m), and  $\phi_h$  is a diabatic correction factor dependent on the Richardson number computed from  $H$ . Use of an alternative expression employed by van de Griend and

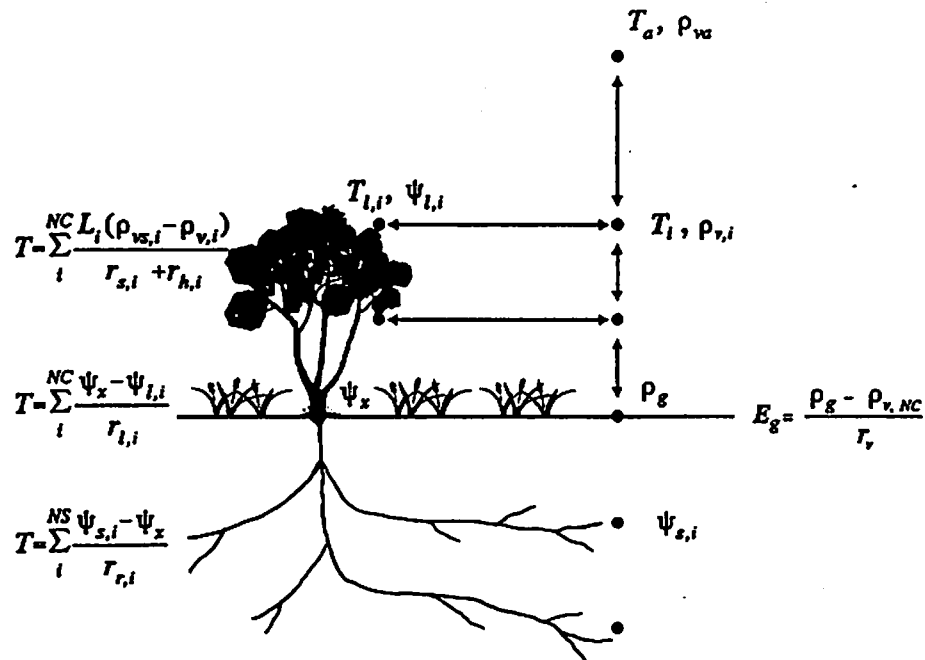


FIG. 2. Physical representation of water flow through a plant in response to transpiration demands. (Here  $\rho_x$  is vapor density at the ground surface, and  $r_x$  is resistance to vapor transfer within the canopy and equal to  $\Delta z/k_x$ ; all other symbols are defined in the text.)

van Boxel (1989), Nichols (1992), and Huntingford et al. (1995) is discussed in the appendix.

Heat transfer from the vegetation elements (leaves) to the air space within a canopy layer for a given plant species ( $\text{W m}^{-2}$ ) is computed from

$$H_{l,i} = -\rho_a c_a L_i \frac{(T_{l,i} - T_i)}{r_{h,i}}. \quad (8)$$

Here,  $L_i$ ,  $T_{l,i}$ , and  $T_i$  are leaf area index, leaf temperature, and air temperature within canopy layer  $i$ , and resistance to convective transfer from the canopy leaves per unit leaf area index,  $r_{h,i}$ , is computed from (Campbell 1977)

$$r_{h,i} = 307 \left( \frac{d_i}{u_i} \right)^{1/2}, \quad (9)$$

where  $d_i$  is leaf dimension (m),  $u_i$  is wind speed within the canopy layer ( $\text{m s}^{-1}$ ), and 307 is a coefficient ( $\text{s}^{1/2} \text{m}^{-1}$ ) for the thermal diffusivity and viscosity of air. Leaf temperature for each layer within the canopy ( $T_{l,i}$ ) is determined from a leaf energy balance of the canopy layer, assuming the leaves within the canopy have negligible heat capacity:

$$R_{n,i} + H_{l,i} + L_v E_{l,i} = 0. \quad (10)$$

Here,  $R_{n,i}$  is net all-wave radiation for the leaf surfaces within canopy layer  $i$  for a given plant species ( $\text{W m}^{-2}$ ). Water uptake, transpiration, and leaf temperature are coupled through the energy balance of the leaf, which is calculated for each plant species within each canopy layer. The leaf energy balance is computed iteratively

with heat and water vapor transfer equations [Eqs. (4) and (5)] and transpiration within the canopy.

Transpiration within a canopy layer,  $E_{l,i}$  ( $\text{W m}^{-2}$ ), is determined assuming a soil-plant-atmosphere continuum. Water flow is calculated assuming continuity in water potential throughout the plants, as illustrated in Fig. 2, and may be calculated at any point in the plant from

$$T = \sum_{m=1}^{NS} \frac{\psi_{s,m} - \psi_x}{r_{r,m}} = \sum_{i=1}^{NC} \frac{\psi_x - \psi_{l,i}}{r_{l,i}} = \sum_{i=1}^{NC} \frac{\rho_{v,s,i} - \rho_{v,i}}{r_{s,i} + r_{h,i}} L_i. \quad (11)$$

Here,  $T$  is total transpiration rate ( $\text{kg m}^{-2} \text{s}^{-1}$ ) for a given plant species;  $\psi_{s,m}$ ,  $\psi_x$ , and  $\psi_{l,i}$  are water potential (m) in layer  $m$  of the soil, in the plant xylem, and in the leaves of canopy layer  $i$ ;  $r_{r,m}$  and  $r_{l,i}$  are the resistance to water flow ( $\text{m}^3 \text{s kg}^{-1}$ ) through the roots of layer  $m$  and the leaves of layer  $i$ ;  $\rho_{v,s,i}$  and  $\rho_{v,i}$  are the vapor density ( $\text{kg m}^{-3}$ ) within the stomatal cavities (assumed to be saturated vapor density) and of the air within the canopy layer;  $r_{s,i}$  is stomatal resistance per unit of leaf area index ( $\text{s m}^{-1}$ );  $NS$  and  $NC$  are the number of soil and canopy nodes; and other terms are as described previously. Root resistance for each plant species within each soil layer is calculated by dividing total root resistance for the plant by its fraction of roots within the soil layer. Leaf resistance for each plant species within each canopy layer is computed from total leaf resistance for the plant based on its leaf area index within each canopy layer. Transpiration from the leaves of each plant species within each canopy layer,  $E_{l,i}$ , is computed from the last term in Eq. (11).

Water flow within the plant is controlled mainly by changes in stomatal resistance. A simple equation relating stomatal resistance to leaf water potential is (Campbell 1985)

$$r_s = r_{s0} [1 + (\psi_l / \psi_c)^n], \quad (12)$$

where  $r_{s0}$  is stomatal resistance ( $\text{m s}^{-1}$ ) with no water stress (assumed constant),  $\psi_c$  is a critical leaf water potential (m) at which stomatal resistance is twice its minimum value, and  $n$  is an empirical coefficient that has typically been set to 5 (Flerchinger et al. 1996b; Flerchinger and Pierson 1997). Sensitivity of model simulations to stomatal resistance parameters was presented by Flerchinger and Pierson (1997). Equations relating stomatal resistance to leaf temperature, vapor pressure deficit, soil moisture deficit, and solar irradiance have been developed (e.g., Dolman 1993; Mihailović and Ruml 1996); however, estimation of a separate parameter is required for each of these factors. Because these factors all have an indirect effect on leaf water potential, Eq. (12) is very effective in estimating stomatal resistance. Although Eq. (12) does not account for direct effects of extreme temperature or solar radiation on plant stress, the plants considered in the present study are well adapted to the hot, arid conditions encountered at the study sites.

### 3. Site description

The study site was located near Tucson, Arizona, within the Walnut Gulch experimental watershed (approximately  $150 \text{ km}^2$  in size) operated by the U.S. Department of Agriculture's Agricultural Research Service (USDA ARS) Southwest Watershed Research Center. Data was collected as part of the Monsoon '90 multidisciplinary large-scale field campaign described by Kustas and Goodrich (1994). The field experiment was designed to measure many aspects of the hydrologic response of a semiarid watershed to midsummer monsoon rainfall.

The main field campaign was conducted during July–August 1990, during which a network of eight meteorological stations (METFLUX sites) was installed across the  $150\text{-km}^2$  Walnut Gulch watershed. More extensive remote sensing and hydrometeorological measurements were collected at METFLUX sites 1 and 5, known as the Lucky Hills and Kendall sites, respectively, located within the two dominant vegetation types that exist within the Walnut Gulch watershed. The Lucky Hills subwatershed is  $4.5 \text{ ha}$ , and the Kendall subwatershed covers  $60 \text{ ha}$ . Kustas et al. (1994) and Stannard et al. (1994) described the surface energy flux measurements. The Lucky Hills site, representative of the shrub-dominated ecosystem located primarily in the western part of the watershed, consists largely of creosote bush (*Larrea tridentata*) spaced 2–5 m apart (25% cover) separated by essentially bare interspace areas. Vegetation cover at the grass-dominated Kendall site located in the eastern part of the watershed is more ho-

mogeneous with around 40% cover during the monsoon season (Weltz et al. 1994).

### 4. Field measurements

Data collected at the Lucky Hills and Kendall sites consisted of continuous meteorological measurements, near-surface soil temperature and moisture, canopy temperature, and surface energy fluxes. Surface flux measurements were collected using a Bowen ratio, eddy correlation, and variance techniques (Kustas et al. 1994; Stannard et al. 1994). To obtain a continuous record of surface flux estimates for comparison with model predictions,  $H$  was estimated using variance methods with measurements of  $R_n$  and  $G$ , and solving for  $L_v E$  as a residual of Eq. (1) at Kendall and Lucky Hills. This variance-residual approach is described in detail by Kustas et al. (1994). A flux source area analysis performed by Kustas and Humes (1997) indicated variance-residual flux observations were representative of approximately a 400-m upwind fetch depending on windspeed; the contributing area to the METFLUX stations varied from 0.1 to 1 ha. Canopy and soil surface temperatures were monitored using two Everest Interscience radiometers (model 4000) at each site: one pointed at the soil and the other at the vegetation. Instruments were positioned 1–2 m above the surface. This same instrument setup was used in an earlier study by Nichols (1992). Soil temperature was measured at depths of 2.5, 5, and 15 cm at the METFLUX stations. Additionally, soil temperature and water content were measured at depths of 2.5, 5, 7.5, 10, 20, 30, and 50 cm using thermocouples and time domain reflectometry (TDR) probes installed in trenches near each of the sites. At Lucky Hills, profiles were located in open areas and underneath vegetation, while measurements at the Kendall site were made on north- and south-facing slopes a short distance (100–300 m) from the METFLUX station.

Continuous composite radiometric surface temperatures were not available, but periodic measurements were made over a set of transects using nadir viewing instruments, similar to those used to measure canopy and soil surface temperature, mounted on yoke-type backpacks. Details of the yoke measurements are given by Moran et al. (1994). Regression equations between yoke measurements of composite radiometric surface temperature and measurements of canopy and soil surface temperatures were developed by Norman et al. (1995). The relation for radiometric surface temperature for the Kendall site was

$$T_{\text{rad}} = (0.67 T_s^2 + 0.33 T_c^2)^{1/4} - 273.15, \quad (13)$$

and for the Lucky Hills site it was

$$T_{\text{rad}} = (0.57 T_s^2 + 0.41 T_c^2)^{1/4} - 273.15, \quad (14)$$

where  $T_s$  and  $T_c$  are measured soil surface and canopy temperature ( $^{\circ}\text{C}$ ), respectively. Hourly estimates of composite radiometric surface temperature were computed from the hourly canopy and soil surface temperature measurements. Note that the coefficients weighting  $T_s$  and  $T_c$

TABLE 1. Description and definition and model performance measures.  $\hat{Y}_i$  = simulated values;  $Y_i$  = observed values;  $\bar{Y}$  = mean of observed values.

Measure	Description	Mathematical definition*
ME	Model efficiency, that is, variation in measured values accounted for by the model.	$1 - \frac{\sum_{i=1}^n (Y_i - \hat{Y}_i)^2}{\sum_{i=1}^n (Y_i - \bar{Y})^2}$
rmsd	Root-mean-square difference between simulated and observed values.	$\left[ \frac{1}{n} \sum_{i=1}^n (\hat{Y}_i - Y_i)^2 \right]^{1/2}$
MBE	Mean bias error of model predictions compared to observed values.	$\frac{1}{n} \sum_{i=1}^n (\hat{Y}_i - Y_i)$

for Kendall equal 1.0 and are similar to the respective vegetation and soil cover fractions. For Lucky Hills, the coefficients do not add up to 1.0, and the coefficient for  $T_c$  is significantly higher than the fractional cover for the site (approximately 0.26). This suggests that the observations of soil and vegetation temperature for the Lucky Hills site may contain some bias.

Vegetation properties were measured along five 30.5-m line-intercept transects and included measurements of plant height, canopy diameter, standing biomass, canopy cover, and ground cover by plant species. Ground cover characteristics, including bare soil, rocks, litter, and basal plant area, were estimated using a 20-pin vertical point frequency at randomly located points along the transect (Weltz et al. 1994). Standing biomass was determined by lifeform by clipping 0.5-m<sup>2</sup> areas to a 0.02-m stubble. Both sites were essentially void of surface residues. Rooting distribution with depth was determined from samples collected from the trenches where thermocouples and TDR probes were installed. Typical vegetation height and leaf area index were roughly 0.5 and 0.8 m, respectively, for the Kendall site. Spatially averaged leaf area index for the Lucky Hills site was around 0.4 with the height of the larger shrubs around 1.0 m (Daughtry et al. 1991). Rooting depths were approximately 150 cm at the Kendall site and 120 cm at the Lucky Hills site.

### 5. Model simulations

The model was run from 21 July to 10 August (day 202 to 222) of 1990 for each of the two sites. Simulations using hourly time steps and hourly observations of air temperature, wind speed, relative humidity, solar radiation, and precipitation were carried to a soil depth of 400 cm, where a constant temperature and a unit gradient in water potential (i.e., gravity flow only) were assumed. Temperature at 400 cm was assumed equal to the annual average soil temperature measured within the trenches (19.7° and 19.9°C for Kendall and Lucky Hills, respectively). Two canopy layers and soil nodes at depths of 0, 3, 5, 8, 10, 20, 30, 50, 70, 100, 130, 160, 200, 250, 300, 350, and 400 cm were simulated for each site. Soil temperatures and water contents measured in the trenches were used to initialize the soil profile on day 202 to a depth of 400 cm by extrapolating beyond the 50-cm depth measurements.

Initial water contents were assumed uniform below 50 cm. Each day of simulation required approximately 1 s of computer time using a 90-MHz Pentium processor.

The model was run without prior calibration; however, detailed measurements, values obtained from literature, and prior experience with the model were required to parameterize the model. Measured plant height, leaf area index, and rooting depth were used to parameterize the model. Leaf resistance ( $r_l$ ), root resistance ( $r_r$ ), unstressed stomatal resistance ( $r_{so}$ ), and critical leaf water potential ( $\psi_c$ ) for creosote bush were estimated at  $5.6 \times 10^5 \text{ m}^3 \text{ s kg}^{-1}$ ,  $2.4 \times 10^6 \text{ m}^3 \text{ s kg}^{-1}$ ,  $110 \text{ s m}^{-1}$ , and  $-350 \text{ m}$  based on data presented by Meinzer et al. (1988). Total plant resistance for fescue is  $1.15 \times 10^5 \text{ m}^3 \text{ s kg}^{-1}$  (Burch 1979 as cited by Abdul-Jabbar et al. 1984). Root resistance and leaf resistance for grasses were therefore set to  $0.77 \times 10^5 \text{ m}^3 \text{ s kg}^{-1}$  and  $0.38 \times 10^5 \text{ m}^3 \text{ s kg}^{-1}$ , respectively, based on typical ratios of root to leaf resistance. Soil hydraulic properties were estimated from soil texture using the method presented by Campbell (1985).

Because the SHAW model assumes the plant canopy is uniformly distributed horizontally, application of the model to the Lucky Hills site, where there is considerable variability in vegetation between bush-covered and essentially bare interspace areas, obviously violates model assumptions. Thus, surface energy balance simulated for the Lucky Hills site likely represents some areal average of the energy balance; realistically, the surface energy balance for bare versus vegetated areas at the site could be considerably different. However, the model has been applied to similar sites with success (Flerchinger et al. 1996b).

Simulated and measured values of the surface energy balance and canopy and soil temperatures were compared using model efficiency (ME), root-mean-square difference (rmsd), and mean bias error (MBE). Definitions for each are given in Table 1 (Nash and Sutcliffe 1970; Green and Stephenson 1986).

### 6. Model results

Hourly values for the surface energy fluxes for the last 10 days of simulation are plotted in Fig. 3 for the Lucky Hills site. Simulated diurnal variation in each aspect of the energy balance mimicked observed values. Model efficiency, root-mean-square difference, and mean bias error

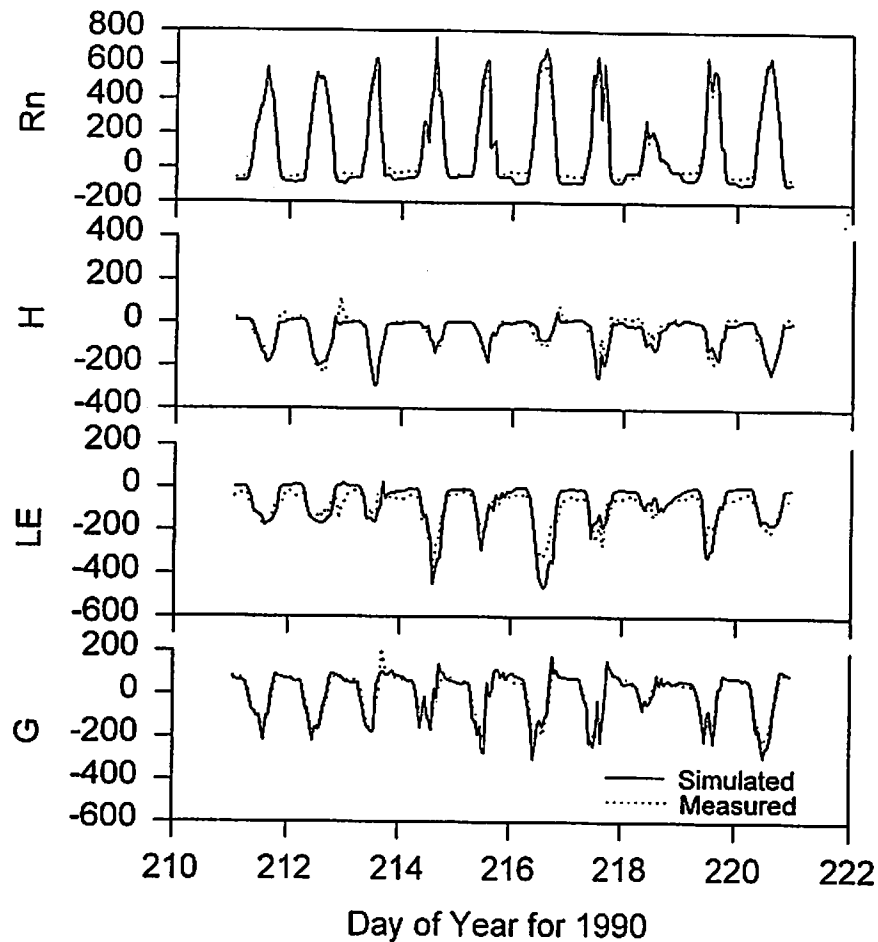


FIG. 3. Times series of simulated and measured surface energy balance ( $W m^{-2}$ ) for the shrub-dominated Lucky Hills site. (Fluxes positive toward the surface.)

comparing simulated net radiation, sensible heat flux, latent heat flux, and ground heat flux with measured values are listed in Table 2. Based only on ME and rmsd, model performance in simulating the hourly surface energy balance was very similar for the two sites, with the exception that ground heat flux was simulated significantly better at the Lucky Hills site. Given the greater heterogeneity of the Lucky Hills site, this is somewhat surprising; however,

TABLE 2. Average measured fluxes, model efficiency (ME), root-mean-square difference (rmsd), and mean bias error (MBE) for the simulated surface energy balance of each site.

Measure	$R_n$	$H$	$L_e E$	$G$
Kendall site				
Average ( $W m^{-2}$ )	153	-45	-111	3
ME	0.98	0.88	0.65	0.71
rmsd ( $W m^{-2}$ )	35	28	56	45
MBE ( $W m^{-2}$ )	-6	3	10	-7
Lucky Hills site				
Average ( $W m^{-2}$ )	137	-40	-95	-2
ME	0.98	0.83	0.59	0.91
rmsd ( $W m^{-2}$ )	33	31	46	30
MBE ( $W m^{-2}$ )	-1	-11	17	-5

Stannard et al. (1994) show good agreement in soil heat flux between the different instrumentation at the Lucky Hills site, whereas there was more variability at the Kendall site. Comparisons of soil heat flux measured by different flux stations yielded an rmsd of  $29 W m^{-2}$  for the Lucky Hills site compared to  $44 W m^{-2}$  for the Kendall site. Thus, with more variability in the measured values of soil heat flux data at the Kendall site, more scatter would be expected when comparing with simulated values. Because the observed latent heat flux values used here were computed by residual from the surface energy balance given in Eq. (1), this uncertainty in soil heat flux would be directly translated to latent heat flux, resulting in a greater rmsd for latent heat flux at the Kendall site.

Further analysis reveals a bias in latent heat flux for both sites, as indicated by MBE in Table 2. Inspection of the plot of simulated versus measured latent heat flux in Fig. 4 reveals that this bias can be attributed primarily to an underprediction of nighttime evapotranspiration compared to measured values. This underprediction of nighttime evapotranspiration (ET) is due in part to a persistent overestimate of nighttime net radiation losses, as shown in Fig. 3. Causes for the bias in simulated nighttime ra-

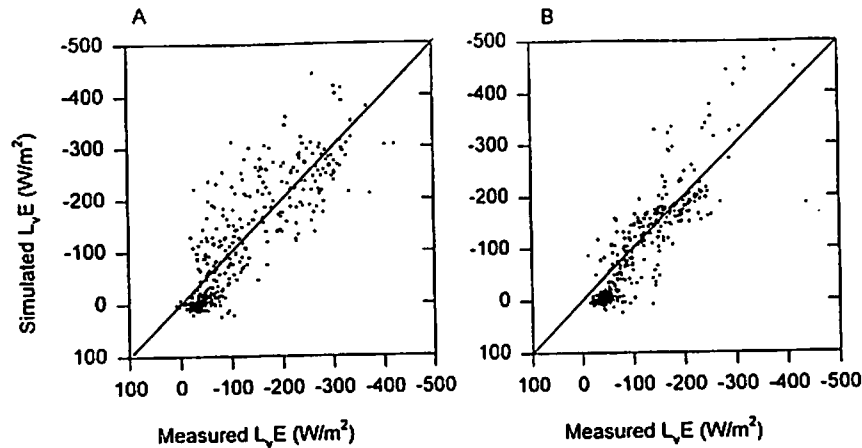


FIG. 4. Simulated vs measured latent heat flux for (a) the grass-dominated Kendall site and (b) the shrub-dominated Lucky Hills site.

diation estimates are unclear, but Flerchinger et al. (1996b) experienced a similar bias at one of three sites simulated in that study. Nevertheless, the underprediction in nighttime evapotranspiration can be attributed in part to a bias in the latent heat flux measurements. Keefer et al. (1997) found that the variance residual technique generally overpredicted the magnitude of nighttime latent heat flux when compared to eddy correlation measurements during periods when both were operating, resulting in a bias in daily ET of approximately 0.3 mm. Adjusting the indirect estimate of ET from the variance technique for this apparent bias, "measured" and simulated ET at Lucky Hills for the 20 days of simulation were 59 and 54 mm, respectively. Measured and simulated ET for the Kendall site were 68 and 71 mm, respectively.

When only daytime fluxes were considered ( $R_n > 100 \text{ W m}^{-2}$ ), latent heat flux was overpredicted (i.e., more negative) for both sites, as shown in Table 3. An MBE of daytime latent heat flux was  $-7 \text{ W m}^{-2}$  for the Lucky Hills and  $-13 \text{ W m}^{-2}$  for the Kendall site. This can largely be attributed to overprediction of daytime  $R_n$  by an average of  $25 \text{ W m}^{-2}$  for the Lucky Hills site and  $27 \text{ W m}^{-2}$  for the Kendall site. The rmsd for  $G$  and  $L_v E$  was higher for the Kendall site, due in part to the uncertainty in measurements of  $G$ .

The largest difference between simulated and estimated daily evapotranspiration common to both sites occurred

TABLE 3. Root-mean-square difference (rmsd) and mean bias error (MBE) for daytime ( $R_n > 100 \text{ W m}^{-2}$ ) simulated surface energy balance of each site.

Measure	$R_n$	$H$	$L_v E$	$G$
Kendall site				
rmsd ( $\text{W m}^{-2}$ )	35	35	73	64
MBE ( $\text{W m}^{-2}$ )	25	13	-13	-25
Lucky Hills site				
rmsd ( $\text{W m}^{-2}$ )	37	39	49	41
MBE ( $\text{W m}^{-2}$ )	27	-12	-7	-8

on day 216 after several rainfall events (Fig. 3). Based on simulated and measured canopy and soil surface temperatures (Fig. 5), this was likely due to an overprediction of soil surface evaporation rather than canopy transpiration. Soil surface temperature was notably underpredicted for this day, which was caused by the model predicting significant evaporative cooling at the soil surface. Midday near-surface (5 cm) soil water contents were overpredicted at both sites, but simulated values rapidly declined by the end of the day in response to the large simulated evaporation demand.

Air temperature, simulated and measured canopy leaf temperature, and soil surface temperature are plotted in Fig. 5 for the Kendall site. Measured canopy and soil surface temperatures were obtained from the IRT sensors. Model efficiency, rmsd, and MBE comparing simulated and measured temperatures are listed in Table 4. Model performance was similar for the two sites with the excep-

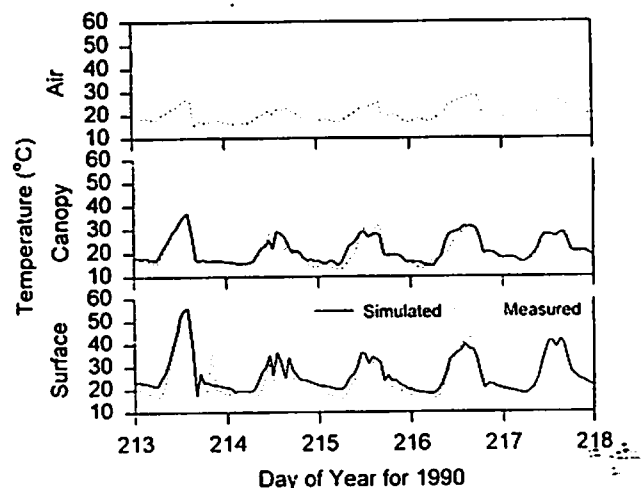


FIG. 5. Time series of air temperature, and simulated and measured canopy and soil surface temperature ( $^{\circ}\text{C}$ ) for the grass-dominated Kendall site.

tion that canopy leaf temperature for the Lucky Hills site had a positive bias of 1.8°C, as illustrated in Fig. 6, compared to 0.8°C for the Kendall site. The fact that the bias is consistent regardless of the magnitude and direction of latent and sensible heat fluxes suggests that it is probably not related to within-canopy transfer processes. At both sites, simulated midday leaf temperatures were typically 6°C higher than air temperature. This roughly mimicked measured leaf temperatures at the Kendall site, but measured midday leaf temperatures at the Lucky Hills site were only a couple of degrees higher than air temperature (Fig. 5). There could be a bias in the IRT measurements, especially for the Lucky Hills site where coefficients in (16) do not add up to unity and are not representative of the fractional cover. The large bias in simulated radiometric surface temperature for the Lucky Hills site compared to estimated values (Table 4) may be related to the limitation of the model in assuming a uniform vegetation cover.

To illustrate the utility of using remotely sensed data to verify and update the model, day 216 was run with varying stomatal resistances and soil water contents. The model was run using the relatively wet soil water profile present on day 216 and drier conditions present prior to the precipitation events. Stomatal resistance parameters were adjusted to obtain varying stomatal resistances for each soil moisture condition. Stomatal resistance is plotted against radiometric surface temperature for both sites in Fig. 7. The data fall into two regimes dictated by soil water content. The large difference in radiometric surface temperature between the wet and dry profiles is due to soil surface temperature, which differed by up to 15°C between soil moisture conditions. Radiometric surface temperature had little variation with stomatal resistance for the moist soil condition but had somewhat more variation under dry conditions. Thus, with known soil moisture conditions and relatively dry surface conditions (see discussion to follow), model parameters can potentially be adjusted to fine-tune the simulated radiometric surface temperature and thus transpiration rate.

Unfortunately, available methods for remotely sensing soil moisture are effective for only the surface 5 cm, making soil moisture for the entire soil profile difficult to obtain. Therefore, additional model runs were made with a relatively wet ( $0.40 \text{ m}^3 \text{ m}^{-3}$ ) and dry ( $0.05 \text{ m}^3 \text{ m}^{-3}$ ) soil

water contents in the top 5 cm. Water content within the root zone was varied from 0.05 to  $0.40 \text{ m}^3 \text{ m}^{-3}$  for each surface soil moisture conditions and plotted against the resulting radiometric surface temperature in Fig. 8. As with Fig. 7, there was relatively little difference in radiometric surface temperature with moist surface conditions due to the dominance of the evaporative cooling of the soil surface. However, under dry surface conditions, there was considerably more sensitivity of radiometric surface temperature with soil moisture. Thus, with a combination of remotely sensed surface soil water content provided by a microwave sensor (Schmugge et al. 1994) and radiometric surface temperature, Fig. 8 potentially provides a method to estimate soil moisture at depth and to verify, track, and periodically update model simulations for sparse canopies.

## 7. Summary and conclusions

The Simultaneous Heat and Water (SHAW) model is a process model of heat and water transfer through a plant-snow-residue-soil system that integrates the detailed physics of heat and water transfer through plant cover, snow, residue, and soil into one model. The numerical approach used by the model to simulate the surface energy balance and within-canopy transfer processes is presented. The SHAW model was applied to data collected as part of the Monsoon '90 multidisciplinary field experiment to test the model's ability to simulate heat and water fluxes and surface temperatures for two diverse vegetation communities in the semiarid southwestern United States. The model was applied to two 400-cm profiles: one located at a grass-dominated site having uniform, albeit sparse plant cover, and another situated in a heterogeneous shrub-dominated location having considerable bare soil areas between shrubs. Diurnal variation in simulated surface energy budgets mimicked observed values.

Model performance was similar for the two sites. The magnitude of daytime latent and soil heat fluxes were overpredicted at both sites, partially due to overprediction in net radiation by approximately  $25 \text{ W m}^{-2}$ . Evaporation from the soil surface was likely overpredicted at both sites shortly after rainfall events. However, simulated latent heat flux and ground heat flux displayed more scatter for the grass-dominated site. Root-mean-square differences in the daytime values at the grass-dominated site were  $73 \text{ W m}^{-2}$  for latent heat flux and  $64 \text{ W m}^{-2}$  for ground heat flux, compared to  $49 \text{ W m}^{-2}$  for latent heat flux and  $41 \text{ W m}^{-2}$  for ground heat flux at the shrub-dominated site. This was partially attributed to uncertainty in soil heat flux at the grass-dominated site. Additionally, simulated canopy leaf temperature for the shrub-dominated site had a positive bias of 1.8°C. Mean bias error in simulated soil surface temperature and 2.5-cm soil temperature ranged from 0.6° to 0.9°C at both sites.

Based on simulation results, the SHAW model can reasonably simulate the surface energy balance and canopy temperatures over diverse vegetation communities, including sparse, heterogeneous plant canopies. The model

TABLE 4. Model efficiency (ME), root-mean-square difference (rmsd), and mean bias error (MBE) for simulated canopy, soil surface, 2.5-cm soil, and composite radiometric surface temperatures.

Measure	$T_c$	$T_s$	$T_{2.5\text{cm}}$	$T_{\text{rad}}$
Kendall site				
ME	0.93	0.94	0.74	0.94
rmsd (°C)	1.8	2.6	3.0	2.3
MBE (°C)	0.8	0.9	-0.9	0.6
Lucky Hills site				
ME	0.80	0.94	0.71	0.75
rmsd (°C)	2.3	2.8	3.2	4.6
MBE (°C)	1.8	0.6	0.9	3.9

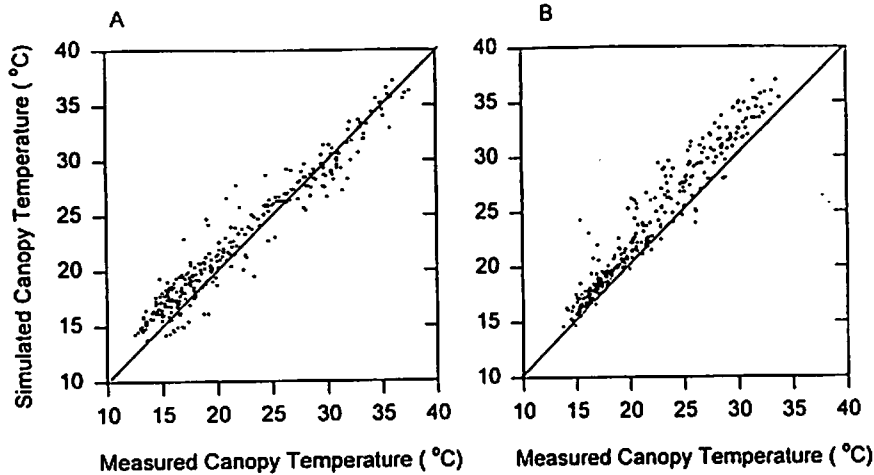


FIG. 6. Simulated vs measured canopy leaf temperature for (a) the grass-dominated Kendall site and (b) the shrub-dominated Lucky Hills site.

may be used to extrapolate fluxes to other areas within the watershed using remote sensing data to estimate model inputs such as leaf area index and fractional vegetation cover (Choudhury et al. 1994). The ability of the model to simulate canopy and surface temperatures gives it the potential for being verified and periodically updated using satellite observations of radiometric surface temperature as long as biases in the radiometric observations can be minimized (Cooper et al. 1995). A methodology is proposed whereby a combination of model simulations and remotely sensed radiometric surface temperature and surface soil moisture can be used to estimate root zone soil water content.

**Acknowledgments.** The cooperation and assistance of the USDA ARS Southwest Watershed Research Center in Tucson, Arizona, and on-site personnel who maintained the Walnut Gulch Experimental Watershed during the Monsoon '90 experiment are gratefully acknowledged. Processing of the yoke data was performed by T. R. Clarke and M. S. Moran from the USDA ARS U.S. Water Conservation Laboratory in Phoenix, Arizona. The continuous measurements of soil and vegetation temperatures were collected and processed by W. D. Nichols from the USGS Water Resources Division in Carson City, Nevada. The authors also acknowledge David I. Stannard from the U.S. Geological Survey in Denver, Colorado, and James H.

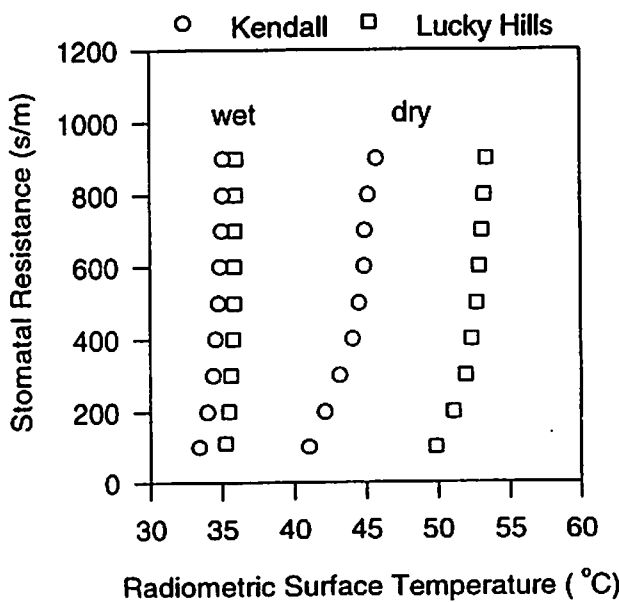


FIG. 7. Effect of midday stomatal resistance on simulated radiometric surface temperature for day 216 using two different soil moisture conditions.

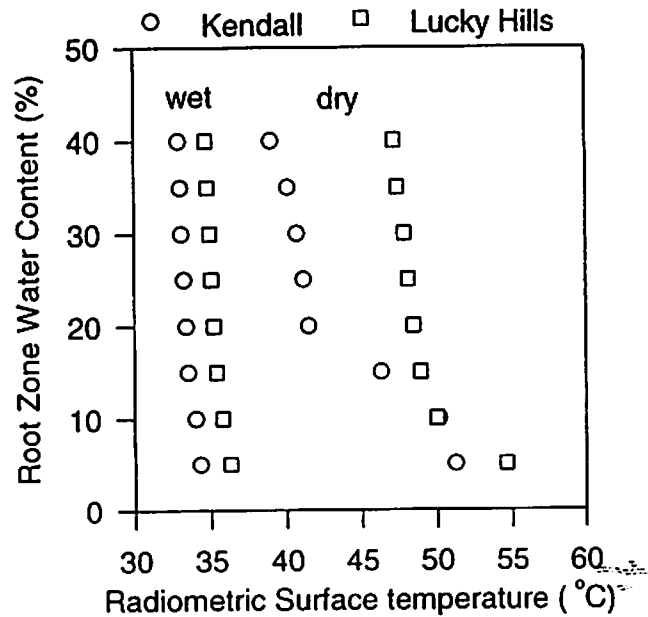


FIG. 8. Effect of soil water content within the root zone on simulated radiometric surface temperature for day 216 using two different surface soil moisture conditions.

Blanford, affiliated with the University of Arizona during Monsoon '90, who were mainly responsible for the surface flux data. Funding from NASA Interdisciplinary Research Program in Earth Sciences (NASA reference IDP-88-086) and funds from USDA ARS Beltsville Area Office provided the necessary financial support to conduct the field study.

## APPENDIX

## Alternate Expression for Transfer within the Canopy

A commonly employed expression for transfer within the canopy is obtained by relating the eddy diffusivity to wind speed within the canopy, which is assumed to decay exponentially (see van de Griend and van Boxel 1989; Nichols 1992; Huntingford et al. 1995). The resistance to heat and vapor transfer between heights  $z_1$  and  $z_2$  ( $z_1 < z_2$ ) within the canopy can be expressed by

$$r_a = \int_{z_1}^{z_2} \frac{1}{K(h)e^{-n(h-z)}} dz = \frac{he^n}{nK(h)} [e^{-nz_1/h} - e^{-nz_2/h}], \quad (\text{A1})$$

where  $n$  is the extinction coefficient for wind speed within the canopy with observed values in the range of 2.5 (Huntingford et al. 1995), and

$$K(h) = \frac{ku_*(h-d)}{\phi_h}. \quad (\text{A2})$$

For a single canopy layer, Eq. (A1) yields values of  $1/r_a$ , approximately twice that of  $k/(\Delta z)$  from Eqs. (6) and (7). Substituting Eq. (A1) for Eqs. (6) and (7) had a detrimental effect on model performance. Model efficiency dropped from 0.88 to 0.78 for sensible heat flux and from 0.65 and 0.62 for latent heat flux at the Kendall site; model efficiency for the Lucky Hills site dropped from 0.83 to 0.46 and from 0.59 to 0.47. Errors in simulated canopy and soil surface temperature also increased by up to 0.8°C in rmsd. Simulations using Eq. (A1) could be improved by using a value for  $n$  greater than typically reported, but  $n$  for the sparse canopies would realistically be lower than that for more dense canopies. Application of Eq. (A1) to sites simulated with the SHAW model by Flerchinger et al. (1996b) also had a detrimental effect on simulated energy fluxes when compared to measured values.

## REFERENCES

- Abdul-Jabbar, A. S., D. G. Lugg, T. W. Sammis, and L. W. Gay, 1984: A field study of plant resistance to water flow in alfalfa. *Agron. J.*, **76**, 765-769.
- Blyth, E. M., and R. J. Harding, 1995: The application of aggregation models of surface heat flux from the Sahelian tiger bush. *Agric. Forest Meteorol.*, **72**, 213-235.
- Burch, G. J., 1979: Soil and plant resistances to water absorption by plant root systems. *Aust. J. Agric. Res.*, **30**, 279-292.
- Burke, E. J., R. J. Gurney, L. P. Simmonds, and T. J. Jackson, 1997: Calibrating a soil water and energy budget model with remotely sensed data to obtain quantitative information about the soil. *Water Resour. Res.*, **33**, 1689-1697.
- Campbell, G. S., 1977: *An Introduction to Environmental Biophysics*. Springer-Verlag, 159 pp.
- , 1985: *Soil Physics with BASIC: Transport Models for Soil-Plant Systems*. Elsevier, 150 pp.
- Choudhury, B. J., N. U. Ahmed, S. B. Idso, R. J. Reginato, and C. S. T. Daughtry, 1994: Relations between evaporation coefficients and vegetation indices by model simulations. *Remote Sens. Environ.*, **50**, 1-17.
- Cooper, H. J., E. A. Smith, and W. L. Crosson, 1995: Limitations in estimating surface sensible heat fluxes from surface and satellite radiometric skin temperatures. *J. Geophys. Res.*, **100**, 25 419-25 427.
- Daughtry, C. S. T., M. A. Weltz, E. M. Perry, and W. P. Dulaney, 1991: Direct and indirect estimates of leaf area index. Preprints, *10th Conf. on Biometeorology and Aerobiology and Special Session on Hydrometeorology*, Salt Lake City, UT, Amer. Meteor. Soc., 230-233.
- Denmead, O. T., and E. F. Bradley, 1985: Flux-gradient relationships in a forest canopy. *The Forest-Atmosphere Interaction*, B. Hutchison and B. B. Hicks, Eds., D. Reidel, 412-442.
- Dolman, A. J., 1993: A multiple source land surface energy balance model for use in GCMs. *Agric. Forest Meteorol.*, **65**, 21-45.
- , and J. S. Wallace, 1991: Lagrangian and K-theory approaches in modelling evaporation and sparse canopies. *Quart. J. Roy. Meteor. Soc.*, **117**, 1325-1340.
- Dickinson, R. E., A. Henderson-Sellers, P. J. Kennedy, and M. F. Wilson, 1986: Biosphere-Atmosphere Transfer Scheme (BATS) for the NCAR Community Climate Model. NCAR Tech. Note 275+STR, National Center for Atmospheric Research, Boulder, CO, 69 pp.
- Flerchinger, G. N., and K. E. Saxton, 1989: Simultaneous heat and water model of a freezing snow-residue-soil system 1. Theory and development. *Trans. Amer. Soc. Agric. Engr.*, **32**, 565-571.
- , and F. B. Pierson, 1991: Modeling plant canopy effects on variability of soil temperature and water. *Agric. Forest Meteorol.*, **56**, 227-246.
- , and —, 1997: Modeling plant canopy effects on variability of soil temperature and water: Model calibration and validation. *J. Arid Environ.*, **35**, 641-653.
- , J. M. Baker, and E. J. A. Spaans, 1996a: A test of the radiative energy balance of the SHAW model for snowcover. *Hydrol. Proc.*, **10**, 1359-1367.
- , C. L. Hanson, and J. R. Wight, 1996b: Modeling evapotranspiration and surface energy budgets across a watershed. *Water Resour. Res.*, **32**, 2539-2548.
- Goudriaan, J., 1989: Simulation of micrometeorology of crops, some methods and their problems, and a few results. *Agric. Forest Meteorol.*, **47**, 239-258.
- Green, I. R. A., and D. Stephenson, 1986: Criteria for comparison of single event models. *Hydrol. Sci. J.*, **31**, 395-411.
- Henderson-Sellers, A., J. Pitman, P. K. Love, P. Irannejad, and T. H. Chen, 1995: The project for intercomparison of land surface parameterization schemes (PILPS): Phases 2 and 3. *Bull. Amer. Meteor. Soc.*, **76**, 489-503.
- Horton, R., 1989: Canopy shading effects on soil heat and water flow. *Soil Sci. Soc. Amer. J.*, **53**, 669-679.
- Huntingford, C., S. J. Allen, and R. J. Harding, 1995: An intercomparison of single and dual-source vegetation-atmosphere transfer models applied to transpiration from Sahelian savanna. *Bound.-Layer Meteorol.*, **74**, 397-418.
- Inclan, M. G., and R. Forkel, 1995: Comparison of energy fluxes calculated with the Penman-Monteith equation and the vegetation models SiB and Cupid. *J. Hydrol.*, **166**, 193-211.
- Keefer, T. W., Kustas, D. Goodrich, and K. Quast, 1997: Estimating water use by semiarid rangeland vegetation during the summer in Southern Arizona. Preprints, *13th Conf. on Hydrology*, Long Beach, CA, Amer. Meteor. Soc., 151-154.
- Kustas, W. P., and D. C. Goodrich, 1994: Preface. Special section: Monsoon '90 multidisciplinary experiment. *Water Resour. Res.*, **30**, 1211-1225.

- , and J. M. Norman, 1996: Use of remote sensing for evapotranspiration monitoring over land surface. *Hydrol. Sci. J.*, **41**, 495–516.
- , and K. S. Humes, 1997: Spatially distributed sensible heat flux over a semiarid watershed. Part II: Use of a variable resistance approach with radiometric surface temperature. *J. Appl. Meteor.*, **36**, 293–301.
- , M. S. Moran, K. S. Humes, D. I. Stannard, P. J. Pinter Jr., L. E. Hipps, E. Swiatek, and D. C. Goodrich, 1994: Surface energy balance estimates at local and regional scales using optical remote sensing from an aircraft platform and atmospheric data collected over semiarid rangelands. *Water Resour. Res.*, **30**, 1241–1259.
- Lagouarde, J. P., Y. H. Kerr, and Y. Brunet, 1995: An experimental study of angular effects on surface temperature for various plant canopies and bare soils. *Agric. Forest Meteorol.*, **77**, 167–190.
- Lascano, R. J., C. H. M. van Bavel, J. L. Hatfield, and D. R. Upchurch, 1987: Energy and water balance of a sparse crop: Simulated and measured soil and crop evaporation. *Soil Sci. Soc. Amer. J.*, **51**, 1113–1121.
- Luo, Y., R. S. Loomis, and T. C. Hsiao, 1992: Simulation of soil temperature in crops. *Agric. Forest Meteorol.*, **61**, 23–38.
- Massman, W. J., 1992: A surface energy balance method for partitioning evapotranspiration data into plant and soil components for a surface with partial canopy cover. *Water Resour. Res.*, **28**, 1723–1732.
- Meinzer, F. C., M. R. Sharifi, E. T. Nilsen, and P. W. Rundel, 1988: Effects of manipulation of water and nitrogen regime on the water relations of the desert shrub *Larrea tridentata*. *Oecologia*, **77**, 480–486.
- Mihailović, D. T., and M. Ruml, 1996: Design of land-air parameterization scheme (LAPS) for modelling boundary layer surface processes. *Meteor. Atmos. Phys.*, **58**, 65–81.
- Moran, M. S., W. P. Kustas, A. Vidal, D. I. Stannard, J. H. Blanford, and W. D. Nichols, 1994: Use of ground-based remotely sensed data for surface energy balance evaluation of a semiarid rangeland. *Water Resour. Res.*, **30**, 1339–1349.
- Nash, J. E., and J. V. Sutcliffe, 1970: River flow forecasting through conceptual models: Part I: A discussion of principles. *J. Hydrol.*, **44**, 282–290.
- Nichols, W. D., 1992: Energy budgets and resistances to energy transport in sparsely vegetated rangeland. *Agric. Forest Meteorol.*, **60**, 221–247.
- Norman, J. M., W. P. Kustas, and K. S. Humes, 1995: A two source approach for estimating soil and vegetation energy fluxes from observations of directional radiometric surface temperature. *Agric. Forest Meteorol.*, **77**, 263–293.
- Raupach, M. R., 1989: A practical Langrangian method for relating scalar concentrations to source distributions in vegetation canopies. *Quart. J. Roy. Meteor. Soc.*, **115**, 609–632.
- Schmugge, T., T. J. Jackson, W. P. Kustas, R. Roberts, R. Parry, D. C. Goodrich, S. A. Amer, and M. A. Weltz, 1994: Push broom microwave radiometer observations of surface soil moisture in Monsoon '90. *Water Resour. Res.*, **30**, 1321–1327.
- Sellers, P. J., W. J. Shuttleworth, J. L. Dorman, J. M. Dalcher, and J. M. Roberts, 1986: A simple biosphere model (SiB) for use within general circulation models. *J. Atmos. Sci.*, **43**, 505–531.
- Stannard, D. I., J. H. Blanford, W. P. Kustas, W. D. Nichols, S. A. Amer, T. J. Schmugge, and M. A. Weltz, 1994: Interpretation of surface flux measurements in heterogeneous terrain during the Monsoon '90 experiment. *Water Resour. Res.*, **30**, 1227–1239.
- van Bavel, C. H. M., R. J. Lascano, and L. Stroosnijder, 1984: Test and analysis of a model of water use by sorghum. *Soil Sci.*, **137**, 443–456.
- van de Griend, A. A., and J. H. van Boxel, 1989: Water and surface energy balance model with a multilayer canopy representation for remote sensing purposes. *Water Resour. Res.*, **25**, 949–971.
- Waggoner, P. E., and W. E. Reifsnyder, 1968: Simulation of the temperature, humidity, and evaporation profiles in a leaf canopy. *J. Appl. Meteorol.*, **7**, 400–409.
- Weltz, M. A., J. C. Ritchie, and H. D. Fox, 1994: Comparison of laser and field measurements of vegetation and canopy cover. *Water Resour. Res.*, **30**, 1311–1319.